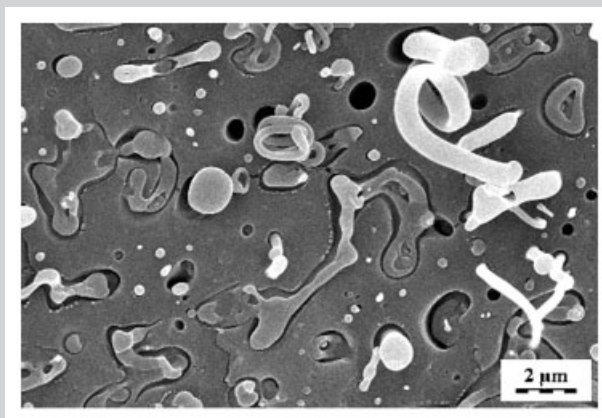


**Full Paper:** The tensile deformation of materials with Poisson's ratio smaller than 0.5 generates an additional free volume, which means that tensile creep under constant stress and temperature is a non-iso-free volume process. Fractional free volume rising proportionally to the creep strain accounts for a continuous shortening of retardation times. To account for this effect, "internal" time has been introduced which is related to a hypothetical pseudo iso-free-volume state. The shift factor along the time scale in the time-strain superposition is not constant for an isothermal creep curve, but rises monotonically from point to point with the elapsed creep time. The reconstructed compliance dependencies obtained for various stresses approximately obey the time-strain superposition thus forming a generalised creep curve. A routinely used empirical equation has been found suitable to describe the effects of time and stress on compliance of parent polymers and their blends. The previously proposed predictive format for the time-dependent compliance of polymer blends has been found applicable also to poly(propylene) (PP)/cycloolefin copolymer (COC) blends with fibrous morphology. As COC shows a tendency to form fibres in a PP matrix, the mixing rule customarily used for fibre composites has been found more appropriate for injection moulded speci-

mens than the equivalent box model for isotropic blends. The predicted compliance curve for a pseudo iso-free-volume state can be transformed into a "real" curve for a selected stress  $\sigma$  (in the interval up to the yield stress).



SEM microphotograph of the fractured surface (perpendicular to the injection direction) of the PP/COC blend 60/40.

## Non-Linear Long-Term Tensile Creep of Poly(propylene)/Cycloolefin Copolymer Blends with Fibrous Structure

Jan Kolařík,\*<sup>1</sup> Alessandro Pegoretti,<sup>2</sup> Luca Fambri,<sup>2</sup> Amabile Penati<sup>2</sup>

<sup>1</sup> Institute of Macromolecular Chemistry, Academy of Sciences of the Czech Republic, 162 06 Prague 6, Czech Republic  
Fax: 420-296809410; E-mail: kolarik@imc.cas.cz

<sup>2</sup> Department of Materials Engineering and Industrial Technologies, University of Trento, 38050 Trento, Italy

Received: January 1, 2003; Revised: May 22, 2003; Accepted: May 22, 2003; DOI: 10.1002/mame.200300005

**Keywords:** compliance; creep; non-linear viscoelasticity; polymer blends; predictive models

### Introduction

The resistance to creep is viewed<sup>[1,2]</sup> as a significant property of polymeric materials whenever end-products are exposed to a long-lasting dead load (constant external force). As generally known, the range of the linear stress-strain relationship of most thermoplastics – in particular of crystalline ones – is rather limited (say a few tenths of %). If the stress exceeds the linearity limit, the produced strain rises more than the acting stress.<sup>[3–9]</sup> Although the creep of many polymers has been described in literature, much less is known about the creep of polymer blends as evidenced

by recent monographs.<sup>[10–15]</sup> Attention has been mainly focused on blends containing a dispersed (discontinuous) minority component;<sup>[10,16–20]</sup> the creep of this type of blends was described in a similar way as that of individual polymers (simple materials). To restrain the creep of a thermoplastic, it is effective to mix it with a creep-resistant polymer that forms a co-continuous component in the resulting binary blend.<sup>[21,22]</sup> The components in heterogeneous binary blends usually assume partial continuity<sup>[23–32]</sup> at a critical volume fraction  $v_{cr}$  in the interval  $0.1 < v_{cr} < 0.3$ ; however,  $v_{cr}$  as low as 0.07 or as high as 0.46 was also reported.<sup>[28,29]</sup>

In our previous papers<sup>[22,33]</sup> we have shown that the stress-strain non-linearity observed in the tensile creep of thermoplastics can be viewed (at least partly) as a consequence of the strain-induced dilatation<sup>[1,8,9]</sup> that occurs in materials with the Poisson ratio  $\nu < 0.5$ . After making correction for the strain-induced fractional free volume, we were able to apply the time-strain superposition successfully to compliance curves (of PP and PP/SAN blends) obtained for a series of stresses.<sup>[22]</sup> Moreover, we have proposed a predictive format for the time-dependent compliance  $D_b(t)$  of heterogeneous binary blends with co-continuous components in the region of linear<sup>[21]</sup> or non-linear<sup>[22,33]</sup> stress-strain relationship.

PP shows a relatively low yield strength and a high propensity to creeping, but preparation of its blends may be rather difficult owing to its limited compatibility with other polymers.<sup>[11]</sup> Compatibilisers generally allow a finer phase structure, higher interface adhesion, lower tendency to phase structure coarsening, enhanced impact resistance, etc., but the resistance to creep depends mainly on the achieved degree of co-continuity of the creep-resistant component. Amorphous ethylene-norbornene copolymers obtained with metallocene-based catalysts<sup>[34,35]</sup> rank among new polymer materials with remarkable properties, such as a high glass transition temperature ( $T_g$ ), transparency, heat resistance, chemical resistance to common solvents, low moisture uptake, high water barrier and good mechanical properties. Available products – usually denoted as cycloolefin copolymers (COC) – have recently attracted much attention in the field of basic and applied material science.<sup>[36–42]</sup> Studies of mechanical properties of ethylene-norbornene copolymers encompass dynamic mechanical thermal analysis (DMTA),<sup>[39,41]</sup> stress-strain measurements,<sup>[39,42]</sup> flexural creep,<sup>[42]</sup> micro-hardness,<sup>[39]</sup> impact strength,<sup>[36]</sup> etc. Because of their olefinic character, COC are likely<sup>[43,44]</sup> to be compatible with polyolefins so that it is worth trying to prepare<sup>[45,46]</sup> PP/COC blends without special compatibilisers. Of available COC products of Ticona<sup>[42]</sup> we have used Topas 8007, i.e., the copolymer with the lowest fraction of norbornene (about 30%), which displays yielding and relatively high strain at break (10%).

Our intention was to prepare blends with the co-continuous “reinforcing” component COC, because numerous studies<sup>[21–24,26,47–51]</sup> have shown that a co-continuous component affects physical properties of blends much more than a dispersed (discontinuous) component. In the case of mechanical properties, a co-continuous “reinforcing” component accounts for higher modulus, yield strength, resistance to creep, etc. Obviously, the effects of this component would be even higher if it could assume the form of fibres. Thus, a number of attempts have recently been made to prepare blends with a fibre-like<sup>[52–54]</sup> or fibrillar<sup>[55–58]</sup> reinforcing component. However, to this end liquid crystalline polymers (LCP) were employed mostly.<sup>[52–54]</sup> Moreover, blend extrudates underwent extensive tensile deformation

(drawing) as the last operation in processing cycle (a more detailed survey is given in ref.<sup>[55]</sup>).

In our previous paper<sup>[45]</sup> dealing with the phase structure of PP/COC blends we have found that in the 90/10, 80/20 and 70/30 blends, the PP matrix contained fibres of COC; the fibre average diameter increased with COC fraction in the range 0.25–0.80  $\mu\text{m}$ . In the 60/40 blend, the COC component formed both fibres (average diameter 2.6  $\mu\text{m}$ ) and larger elongated entities in PP matrix, while the 50/50 blend consisted of co-continuous components. Some COC fibres were broken at the level of fractured surface, which evidences noticeable interface adhesion between PP and COC. The fibre aspect ratio roughly estimated from SEM microphotographs and tensile measurements was at least 20. COC fibres were formed during mixing and/or subsequent injection moulding; the latter process also brought about uniaxial orientation of COC fibres. Unfortunately, it was not possible to systematically vary blend processing conditions to specify their effect on produced morphology (cf. ref.<sup>[53]</sup>). Thus the described fibrous structure was probably obtained thanks to fortuitous coincidence in selecting parent polymers and adjusting processing conditions. The objectives of this paper are (i) to fit non-linear tensile creep of PP/COC blends by a suitable equation, (ii) to apply the time-strain superposition with regard to the strain-induced free volume and (iii) to modify the previously developed predictive format for the creep of fibrous blends.

## Format for Fitting and Prediction of the Non-Linear Creep of Heterogeneous Blends

### Compliance of Thermoplastics

The tensile compliance  $D(t, \sigma, T)$  of polymers, which primarily depends on time  $t$ , stress  $\sigma$  and temperature  $T$ , is customarily viewed as a sum of three components;<sup>[1,2]</sup> (i) elastic (instantaneous)  $D_e(\sigma, T)$ ; (ii) viscoelastic (reversible)  $D_v(t, \sigma, T)$ ; (iii) plastic (irreversible)  $D_p(t, \sigma, T)$ :

$$D(t, \sigma, T) = \varepsilon(t, \sigma, T)/\sigma = D_e(\sigma, T) + D_v(t, \sigma, T) + D_p(t, \sigma, T) \quad (1)$$

where  $\varepsilon(t, \sigma, T)$  is the tensile strain and  $\sigma$  is the tensile stress. The compliance  $D(t, \sigma, T)$  of polymeric materials is most frequently presented in a graphical form. If it can be fitted by a suitable equation, then the storage of experimental data, evaluation of creep rate, interpolation or extrapolation of creep deformation are facilitated. Several attempts have been made<sup>[1,2,59–61]</sup> to introduce factorisation, i.e., to express compliance as a product of three independent functions of time or stress or temperature, i.e.,  $D(t, \sigma, T) = C_p g_1(t) g_2(\sigma) g_3(T)$ . While  $g_3(T)$  is usually identified with the WLF or Arrhenius equation, among numerous empirical functions proposed for  $g_1(t)$  and  $g_2(\sigma)$  we have found<sup>[22,33]</sup> the following equation<sup>[62]</sup> suitable for both short- and

long-term tensile creep of polymer blends:

$$D(t, \sigma) = W(\sigma) (t/\tau_{\text{rm}})^n \quad (2)$$

where  $W(\sigma)$  is a function of the stress,  $\tau_{\text{rm}}$  is the mean retardation time and  $0 \leq n \leq 1$  is the creep curve shape parameter reflecting the distribution of retardation times.

### Effect of Strain-Induced Free Volume on Tensile Creep of Viscoelastic Solids

In this section we will briefly review the format developed in our previous papers.<sup>[22,33]</sup> The effects of temperature and pressure on viscoelastic behaviour of polymers have been successfully interpreted<sup>[1,3-9]</sup> in terms of the dimensionless fractional free volume defined as

$$f = (V - V_h)/V_h \quad (3)$$

where  $V$  is the specific volume,  $V_h$  is the specific volume occupied by molecules (extrapolated from the melt without considering phase changes<sup>[7]</sup>). The expansion of the fractional free volume with increasing (i) temperature (at  $T > T_g$ ) and/or (ii) strain (for solids with the Poisson's ratio  $\nu < 0.5$ ) can be expressed by the following equation:<sup>[1,9,22,33,63-65]</sup>

$$f = f_g + \alpha_{\text{fv}}(T - T_g) + (1 - 2\nu)\varepsilon = f_g + \Delta f_T + \Delta f_\varepsilon \quad (4)$$

where  $f_g$  is the fractional free volume in the glassy state (which is viewed<sup>[1-9]</sup> as an iso-free-volume state with  $f_g = 0.025$ ) and  $\alpha_{\text{fv}} = \alpha_1 - \alpha_g$  is the expansion coefficient of the free volume approximated as the difference between the coefficients above and below  $T_g$ .  $\Delta f_\varepsilon = (1 - 2\nu)\varepsilon$  may constitute a significant contribution to  $f$  in the region of reversible strains smaller than the yield strain.<sup>[33,63-65]</sup>

The available  $f$  controls<sup>[4,64-66]</sup> retardation (or relaxation) times  $\tau_r$  of a polymer:

$$\ln \tau_r = \ln \Omega + (B/f) \quad (5)$$

where  $\Omega$  corresponds to the frequency of thermal motion inside a potential well and  $B \cong 1$  is a numerical factor related to the ratio between the volume of a jumping segment and the volume of critical vacancy necessary for a segment jump. The effect of  $f$  on retardation time  $\tau_r$  can be expressed by means of the shift factor  $\log a$  along the time scale:<sup>[1-9,64-67]</sup>

$$\log a = \log [\tau_r(f_2)/\tau_r(f_1)] \quad (6)$$

where  $f_2 > f_1$ . Combining Equation (5) for the mean retardation time  $\tau_{\text{rm}}$  with Equation (4) and (6), the following equation is obtained for the time-strain shift factor  $\log a_\varepsilon(t)$  defined as the ratio of the retardation times  $\tau_{\text{rm}}[\varepsilon(t), T_c]$  at strain  $\varepsilon(t)$  for time  $t$  and  $\tau_{\text{rm}}[\varepsilon_i = 0, T_c]$  for initial time  $t_i = 0$  (at constant temperature  $T_c$ ):

$$\log a_\varepsilon(t) = -(B/2.303)[(1 - 2\nu)M\varepsilon(t)/(f_g + \Delta f_{Tc})]/[(1 - 2\nu)M\varepsilon(t) + (f_g + \Delta f_{Tc})] \quad (7)$$

where  $M$  is introduced as the ratio of the average strain of the creeping component (or phase) in the test specimen and of the measured strain.

If  $\tau_{\text{rm}}$  of Equation (2) obeys Equation (6), then  $D(t, \sigma)$  can be expressed as

$$\log D(t, \sigma) = [\log W(\sigma) - n \log \tau_{\text{rmi}} - n \log a_\varepsilon(t)] + n \log(t) = \log C(t, \sigma) + n \log t \quad (8)$$

Obviously,  $\log C(t, \sigma)$  rising with the creep time necessarily accounts for an upswing of  $\log D(t, \sigma)$  with  $\log t$ . However, Equation (8) can be reorganised to the following form:

$$\log D(t^*, \sigma) = [\log W(\sigma) - n \log \tau_{\text{rmi}}] + n[\log t - \log a_\varepsilon(t)] = \log C^*(\sigma) + n^* \log t^* \quad (9)$$

where  $t^*$  denotes "internal" time of the creep experiment (asterisk is introduced to indicate that parameters  $C^*$  and  $n^*$  are related to  $t^*$ ):

$$\log t^* = \log t + (B/2.303)[(1 - 2\nu)M\varepsilon(t)/(f_g + \Delta f_{Tc})]/[(1 - 2\nu)M\varepsilon(t)/(f_g + \Delta f_{Tc})] \quad (10)$$

It should be noted that the value of the time-strain shift factor  $\log a_\varepsilon(t)$  is not a constant for an isothermal and iso-stress creep curve, but grows with the creep time due to ever-increasing free volume in the creeping specimen. For this reason, the ratio (experimental time)/(mean retardation time) rises more rapidly than the experimental time itself. The  $\log D(t)$  vs.  $\log t$  plot would coincide with  $\log D(t^*)$  vs.  $\log t^*$  for extremely low stresses and strains ( $\Delta f_\varepsilon \rightarrow 0$ ); thus  $C^*$  and  $n^*$  represent the limiting values of  $C$  and  $n$  for the creep in a (hypothetical) pseudo iso-free volume state.

### Compliance of Heterogeneous Binary Blends in Terms of the Compliance of Components

In the previous papers<sup>[21,22]</sup> we have evaluated the compliance of isotropic heterogeneous polymer blends by combining a two-parameter equivalent box model (EBM) and the data on the phase continuity of components obtained from modified equations of the percolation theory.<sup>[68-70]</sup> Our PP/COC blends containing 0–40% of COC are similar to in situ fibre composites because they consist of a PP matrix and COC fibres. The modulus and inverted value of compliance of blends were found<sup>[45]</sup> to obey the rule of mixing, valid for composites in the direction of uniaxially oriented continuous fibres.<sup>[1,2]</sup> In terms of the compliance of components the rule of mixtures reads

$$1/D_b(t) = \nu_1/D_1(t) + \nu_2/D_2(t) \quad (11)$$

where subscripts 1 and 2 stand for PP and COC, respectively.

Blends with  $50 \leq \% \text{COC} \leq 75$  showing<sup>[45]</sup> partial co-continuity of both components can rather be modelled by means of the equivalent box model (EBM) visualised in Figure 1a, where either constituent consists of a fraction continuous in the direction of the acting force ( $v_{1p}$  or  $v_{2p}$ ) and of a fraction discontinuous in that direction ( $v_{1s}$  or  $v_{2s}$ ). Compliance of the parallel branch  $D_p(t)$  or of the series branch  $D_s(t)$  of the EBM is the following:<sup>[21,22]</sup>

$$1/D_p(t) = v_{1p}/D_1(t) + v_{2p}/D_2(t) \quad (12a)$$

$$1/D_s(t) = (v_{1s} + v_{2s})/[D_1(t)v_{1s} + D_2(t)v_{2s}] \quad (12b)$$

The resulting compliance of blends consisting of two partially co-continuous components is given as the sum of the contributions of the parallel and series branches:

$$D_b(t) = \{v_{1p}/D_1(t) + v_{2p}/D_2(t) + (v_{1s} + v_{2s})^2/[D_1(t)v_{1s} + D_2(t)v_{2s}]\}^{-1} \quad (13)$$

Application of the EBM in the predictive format requires evaluation of the volume fractions  $v_{1p}$ ,  $v_{2p}$ ,  $v_{1s}$  and  $v_{2s}$ . Utilizing a universal formula for elastic modulus (or compliance) proposed by the percolation theory<sup>[68]</sup> for binary

systems, we have derived<sup>[23–29]</sup> the following equations for the volume fractions of the EBM (Figure 1a):

$$v_{1p} = [(v_1 - v_{1cr})/(1 - v_{1cr})]^q \quad (14a)$$

$$v_{2p} = [(v_2 - v_{2cr})/(1 - v_{2cr})]^q \quad (14b)$$

where  $v_{1cr}$  and  $v_{2cr}$  are the critical volume fractions (the percolation thresholds), at which the respective components become partially continuous, and  $q$  is the critical universal exponent. As the EBM in Figure 1a is a two-parameter model, only two of the four volume fractions are independent; thus  $v_{1s} = v_1 - v_{1p}$  and  $v_{2s} = v_2 - v_{2p}$ . To describe the compliance of isotropic binary blends with continuous matrix and one dispersed component (such structures occur in the marginal composition ranges), we have modified<sup>[21]</sup> the Kerner-Nielsen equation<sup>[11]</sup> for modulus of particulate systems. However, as a first approximation, we can consider  $v_{1p} = 0$ ,  $v_{1s} = v_1$  or  $v_{2p} = 0$ ,  $v_{2s} = v_2$  in the EBM. If no experimental data are available for the system under study, the patterns can be predicted by using “universal” values<sup>[68–70]</sup>  $v_{1cr} = v_{2cr} = 0.156$  and  $q = 1.8$ .

### Strain Magnification Factor for the Creeping Component in Heterogeneous Blends

As mentioned above, creep of a polymer 1 can be reduced by blending with a polymer 2 having pronouncedly lower compliance (at the temperature range of envisaged applications). Time-dependent molecular motions underlying creep processes in such a blend then take place mainly in the component (or phase) with higher compliance. To account for a higher strain of the creeping component (phase), we have introduced<sup>[22,33]</sup> the strain-magnifying factor  $M$  defined as the average ratio of the (microscopic) strain in the elements of the creeping component (or phase) and the measured (macroscopic) strain of the creeping specimen. The strain of the fractions  $v_{1p}$  and  $v_{2p}$  coupled in parallel (Figure 1a) is identical with the measured strain, i.e.,  $M_{1p} = M_{2p} = 1$ . On the other hand, if the component 2 has a compliance much lower than component 1, it is evident that the fraction  $v_{2s}$  coupled in series is not strained perceptibly. Consequently, the displacement in the fraction  $v_{1s}$  is equal to the macroscopic displacement, which means that the resulting strain in the fraction  $v_{1s}$  is higher than measured strain.<sup>[22]</sup>

$$M_{1s} = (\Delta L_{1s}/L_{1s})/[(\Delta L_{1s} + \Delta L_{2s})/(L_{1s} + L_{2s})] \quad (15)$$

where  $\Delta L_{1s}$  or  $\Delta L_{2s}$  are the displacements and  $L_{1s}$  and  $L_{2s}$  are the initial lengths (which are proportional to the fractions  $v_{1s}$  and  $v_{2s}$ ). Under the simplifying assumption  $\Delta L_{2s} = 0$  (i.e.,  $M_{2s} = 0$ ), we obtain

$$M_{1s} = (L_{1s} + L_{2s})/L_{1s} = 1 + (v_{2s}/v_{1s}) \quad (16)$$

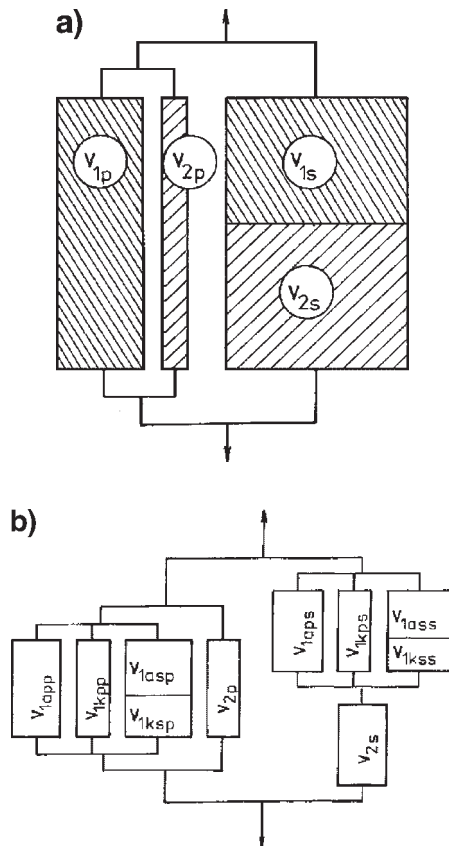


Figure 1. Equivalent box model for a binary blend consisting of (a) amorphous polymers or (b) a crystalline polymer 1 and an amorphous polymer 2.

To include the effect of strain-induced dilatation, we will characterise component 1 by the mean value of  $M_1$ :

$$M_1 = M_{1p}(v_{1p}/v_1) + M_{1s}(v_{1s}/v_1) = (v_{1p}/v_1) + [1 + (v_{2s}/v_{1s})](v_{1s}/v_1) = 1 + (v_{2s}/v_1) \quad (17)$$

To calculate  $M_{1a}$  for amorphous phase in a crystalline polymer, we can substitute subscripts 1 and 2 by "a" (amorphous) and "k" (crystalline), respectively. If a binary isotropic blend consists of a co-continuous crystalline matrix 1 and a co-continuous amorphous polymer 2, it is necessary to introduce a more complex model<sup>[22]</sup> schematically given in Figure 1b, where respective subscripts of the constituting phases are 1a, 1k and 2. The subscripts of fractions of the component 1 combine subscripts p and s in various ways according to the hierarchy of couplings in parallel and/or in series. Following the outlined procedure we can derive<sup>[22]</sup> the average value of  $M_{1a}$  for amorphous phase as the most creeping constituent:

$$M_{1a} = \{v_{1p} + v_{1ksp} + [1 + (v_{2s}/v_{1s})](v_{1s} + v_{1kss})\}/v_{1a} \quad (18)$$

where  $v_{1a}$  stands for the volume fraction of the amorphous phase in component 1. In a similar way we can calculate analogous factors  $M_{1k}$  and  $M_2$ . It can be shown that  $M_{1a} + M_{1k} + M_2 = 1$ , which means that the amount of strain-induced free volume corresponds to the macroscopic strain and that the proposed concept only accounts for an uneven distribution of this free volume. In the case of a crystalline matrix reinforced with unidirectional "long" fibres ( $v_2 \leq 0.4$ ) oriented in the direction of acting tensile stress we can presume that  $v_{2s}$  (Fig. 1b) is negligible, i.e.  $v_{2p} = v_2$ . Then the rising volume fraction of component 2 does not affect the value of  $M_{1a}$  of the amorphous phase in component 1.

## Experimental Part

### Materials

Poly(propylene) Moplen C30G was a product of Basell, Ferrara, Italy: melt flow index (230 °C, 2.16 kg) = 6 ml/min; density: 0.903 g/cm<sup>3</sup>; crystallinity: 52%;  $T_g = -10$  °C. An amorphous cycloolefin copolymer produced under the trade name Topas 8007 was a product of Ticona, Celanese, Germany, consisting of 30% of norbornene units and 70% of ethylene units: MFI = 4.5 ml/10 min; density: 1.02 g/cm<sup>3</sup>;  $T_g = 75$  °C.

### Blend Preparation

A series of PP/COC blends was prepared with 5, 10, 15, 20, 25, 30, 40, 50, 75 wt-% of COC. Polymers were mixed in a Banbury mixer (chamber 4.3 l; 164 rpm) at 190 °C for 3.5 min. The produced pellets were used for feeding a Negri-Bossi injection moulding machine (temperature of the melt 230 °C; barrel temperature 215 °C; injection pressure 30 MPa) to produce dumb-bell test specimens ISO 527 (length: 170 mm;

thickness: 4 mm; gauge length: 80 mm; gauge width: 10 mm). Specimens used for creep studies were stored for more than 6 months at room temperature to avoid any effect of physical ageing during measurements.

### Scanning Electron Microscopy

Scanning electron microscope (SEM) Jeol JSM 6400 was used for studying the phase morphology.<sup>[45]</sup> Samples were fractured in liquid nitrogen perpendicularly to the injection direction and fracture surfaces were covered with platinum using a vacuum sputter (SCD 050, Balzers) before electron microscope examination. SEM microphotographs are the secondary electron images taken at an acceleration voltage of 25 kV. Figure 2a shows a fractured surface with broken COC fibres, while pull-out fibres and more complex COC entities are visualised in Figure 2b.

### Tensile Creep Measurements

The tensile creep was measured by using a simple apparatus equipped with a mechanical stress amplifier (lever) 10:1.

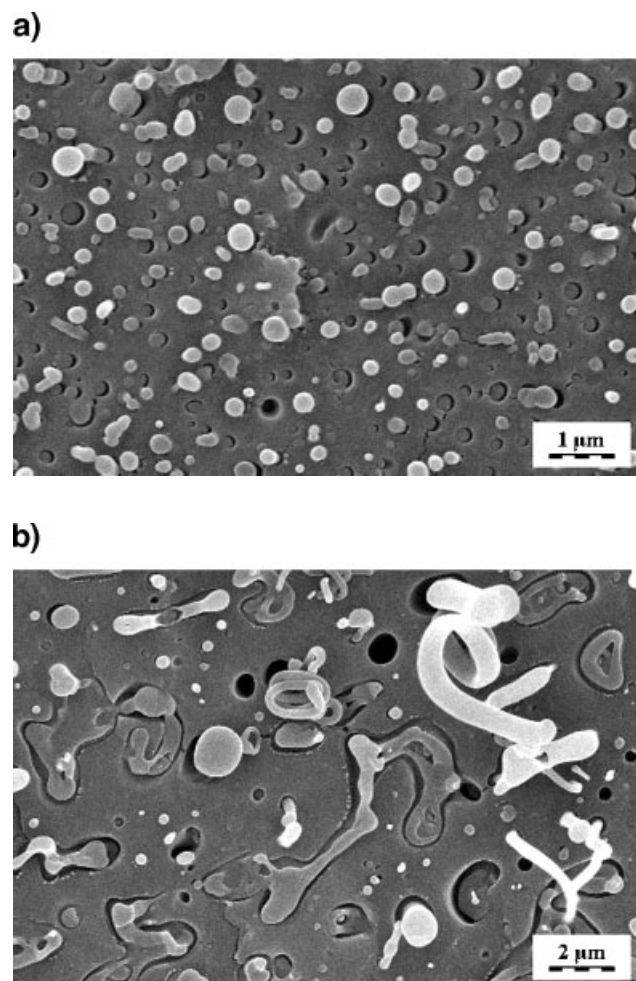


Figure 2. SEM microphotograph of the fractured surface (perpendicular to the injection direction) of the PP/COC blends. (a) PP/COC = 70/30; (b) 60/40.

Short-term tests in the interval 0.1–100 min were performed at four stress levels using one specimen (creep measurement was followed by 22 h recovery). Test specimens were used only once for long-term creep in the interval 0.1–10 000 min. All experiments were performed at room temperature, i.e., 21–23 °C. Mechanical preconditioning consisted in applying a stress (for 1 min) which produced a strain larger than the expected final strain of the intended experiment; the following recovery (before the registered creep was initiated) was about 1 h. Specimen dimensions: initial distance between grips 90 mm; cross-section 10 mm × 4 mm. The length of creeping specimens was measured with the accuracy of 2 μm, i.e., about 0.002%.

## Results and Discussion

### Time-Strain Superposition of Compliance Dependencies Acquired for Different Stresses

The time-strain superposition is illustrated in Figure 3 where the short-term and long-term  $\log D_1(t)$  vs.  $\log t$  or  $\log D_{1v}(t)$  vs.  $\log t$  curves of PP are plotted (Figure 3a, b, c have the

same time axis in order to better visualise the role of the shift factor  $a_e$ ). As long as the effect of strain-induced free volume is neglected ( $M_{1a} = 0$ ) in Figure 3a, increasing stress accounts for (i) an increase in both  $D_1(t)$  and  $D_{1v}(t)$ , (ii) a rising slope of the straight lines roughly approximating  $\log D_1(t)$  vs.  $\log t$  and (iii) an increase in the derivative  $d \log D_1(t)/d \log t$  with the elapsed time of creeping. All these features are usually viewed as evidences of non-linear viscoelastic behaviour. As we have shown previously,<sup>[21]</sup> merely the dependencies  $\log D(t)$  vs.  $\log t$  observed at very low stresses can be well approximated by Equation (2). On the other hand,  $\log D_v(t)$  vs.  $\log t$  plots markedly deviate from a straight line so that a polynomial equation (of the second degree) is necessary to plausibly fit experimental data.

To account for the effect of strain-induced free volume dilatation on creep dependencies, we are to estimate parameters  $M$ ,  $B$ ,  $v$ ,  $T_g$ ,  $f_g$ ,  $\Delta f_{TC}$ ,  $\alpha_{fV}$  occurring in Equation (10). We will employ quantities given for isotactic PP, namely  $T_g = 266$  K,<sup>[7]</sup>  $v = 0.4$ ,<sup>[2]</sup> and  $\alpha_1 - \alpha_g = \alpha_{fV} = 3.3 \cdot 10^{-4} \text{ K}^{-1}$ .<sup>[71]</sup> Employing typical values<sup>[3–5,9]</sup>  $B = 1$  and

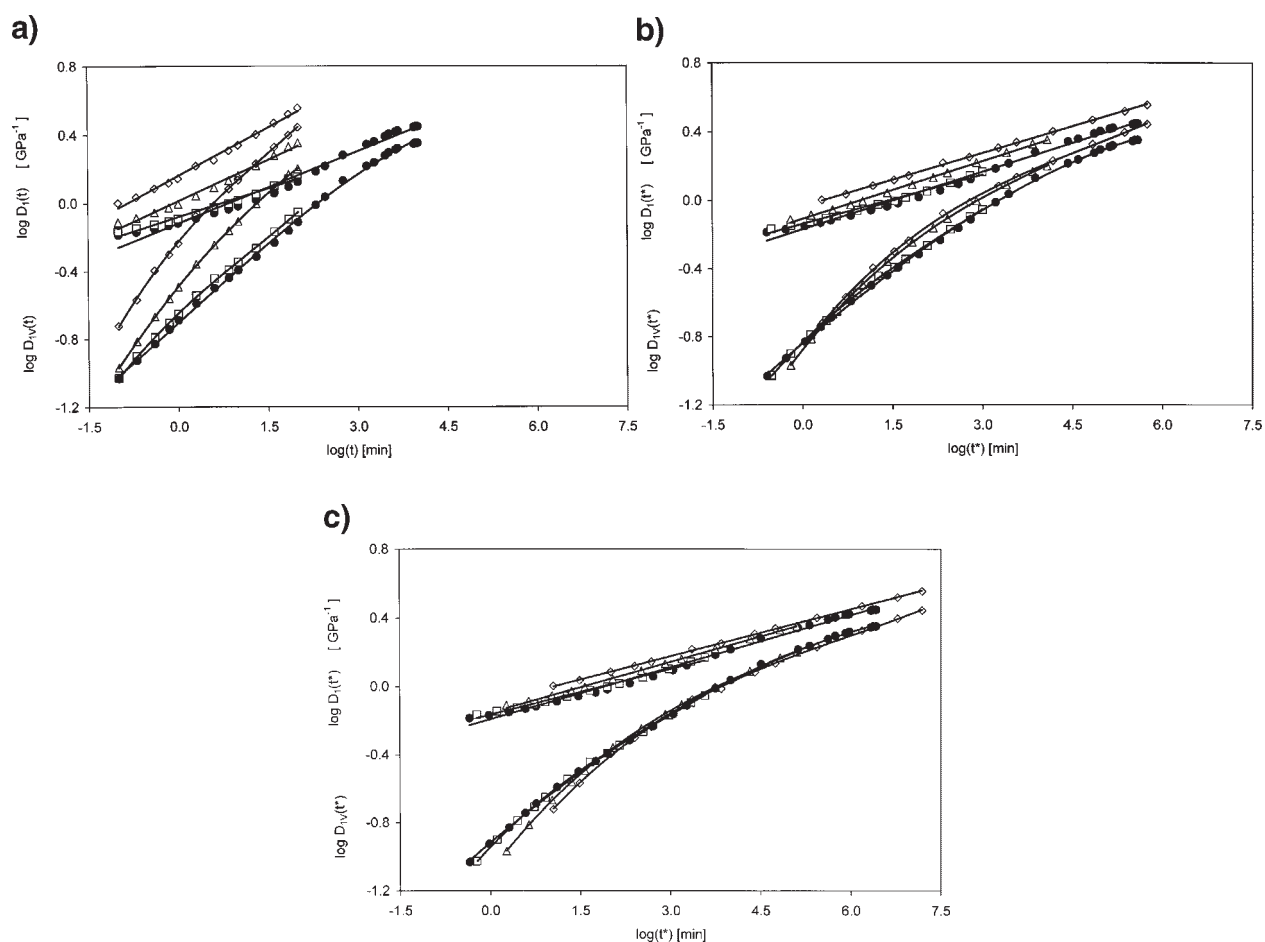


Figure 3. Effect of stress on the compliance  $D(t)$  (upper curves) and viscoelastic component of compliance  $D_v(t)$  (lower curves) of poly(propylene). Applied tensile stress (MPa): short-term creep: ( $\square$ ) 9.80; ( $\triangle$ ) 14.70; ( $\diamond$ ) 19.60; long-term creep: ( $\bullet$ ) 8.55. (a)  $M_{1a} = 0$ ; (b)  $M_{1a} = 1$ ; (c)  $M_{1a} = 1.65$ .

$f_g = 0.025$ , we obtain  $(f_g + \Delta f_{Tc}) = 0.025 + 3.3 \cdot 10^{-4} \text{ K}^{-1}$  (293 K – 266 K)  $\cong 0.034$ . For  $M_{1a} = 1$ , i.e., under a simplified assumption of uniform distribution of the strain-induced free volume throughout the test specimen, the  $\log D(t^*)$  vs.  $\log t^*$  dependencies obtained for various stresses in short-term creeps (Figure 3b) are much closer to one another than in Figure 3a, but still do not well superpose: the rising stress accounts for a slight increase in (i) the compliance  $D(t^*)$  and (ii) the exponent  $n^*$  (Table 1). Also  $\log D_v(t^*)$  grows with acting stress and the dependencies  $\log D_v(t^*)$  vs.  $\log t^*$  markedly deviate from straight lines.

For the studied PP containing about 52% of the crystalline phase,<sup>[72]</sup> Equation (17) provides  $M_{1a} = 1.65$  (using theoretical values  $v_{1cr} = v_{2cr} = 0.156$  and  $q = 1.8$  in the EBM). If this value of  $M_{1a}$  is introduced into Equation (10), i.e., the domination of creep processes in the amorphous phase of PP is considered, the superposition of both  $\log D(t^*)$  vs.  $\log t^*$  and  $\log D_v(t^*)$  vs.  $\log t^*$ , which generally evidences the stress-strain linearity, is fairly good (Figure 3c; Table 1). Disregarding the remaining small effect of stress on  $n^*$ , we can infer that the compliance dependencies determined at stresses far beyond the linearity

Table 1. Effect of the strain-induced free volume on the parameters of Equation (8) and (9): short-term creep.

Stress	$\log C^a)$	$n^a)$	$R^{2c)}$	$\log C^{*b)}$	$n^{*b)}$	$R^{2c)}$	$\log C^{*b)}$	$n^{*b)}$	$R^{2c)}$
MPa									
Poly(propylene)									
	$M = 0^d)$			$M = 1^d)$			$M = 1.65^d)$		
4.90	-0.141	0.092	0.9910	-0.164	0.087	0.9928	-0.177	0.084	0.9937
9.80	-0.081	0.112	0.9812	-0.138	0.096	0.9893	-0.165	0.089	0.9918
14.70	0.013	0.152	0.9863	-0.103	0.108	0.9970	-0.147	0.096	0.9981
19.60	0.173	0.174	0.9933	-0.018	0.099	0.9994	-0.076	0.088	0.9996
Mean	-0.009	0.133	0.9879	-0.106	0.098	0.9946	-0.141	0.089	0.9958
e.s.d. <sup>e)</sup>	0.137	0.038		0.064	0.009		0.045	0.005	
PP/COC = 90/10; $v_2 = 0.09^f)$									
	$M = 0$			$M = 1$			$M = 1.65$		
4.90	-0.190	0.078	0.9964	-0.208	0.075	0.9970	-0.218	0.073	0.9973
9.80	-0.127	0.086	0.9921	-0.168	0.078	0.9945	-0.189	0.073	0.9955
14.70	-0.025	0.120	0.9911	-0.116	0.094	0.9968	-0.155	0.085	0.9978
19.60	0.096	0.137	0.9937	-0.052	0.091	0.9993	-0.104	0.081	0.9996
Mean	-0.062	0.105	0.9933	-0.136	0.085	0.9969	-0.167	0.078	0.9976
e.s.d.	0.125	0.028		0.067	0.009		0.049	0.006	
PP/COC = 85/15; $v_2 = 0.136$									
	$M = 0$			$M = 1$			$M = 1.65$		
4.90	-0.237	0.074	0.9872	-0.252	0.072	0.9887	-0.261	0.070	0.9895
9.80	-0.145	0.079	0.9890	-0.182	0.072	0.9920	-0.201	0.068	0.9932
14.70	-0.091	0.107	0.9784	-0.166	0.088	0.9884	-0.199	0.080	0.9910
19.60	0.024	0.130	0.9733	-0.106	0.091	0.9926	-0.153	0.082	0.9946
Mean	-0.112	0.098	0.9898	-0.177	0.081	0.9904	-0.204	0.075	0.9921
e.s.d.	0.109	0.026		0.060	0.010		0.044	0.007	
PP/COC = 80/20; $v_2 = 0.182$									
	$M = 0$			$M = 1$			$M = 1.65$		
4.90	-0.218	0.068	0.9916	-0.233	0.066	0.9933	-0.241	0.064	0.9930
9.80	-0.163	0.069	0.9916	-0.195	0.064	0.9935	-0.212	0.061	0.9943
14.70	-0.117	0.087	0.9852	-0.177	0.075	0.9911	-0.205	0.070	0.9928
19.60	-0.047	0.108	0.9804	-0.147	0.083	0.9925	-0.188	0.075	0.9944
Mean	-0.136	0.083	0.9872	-0.188	0.072	0.9926	-0.212	0.068	0.9936
e.s.d.	0.072	0.019		0.036	0.009		0.022	0.006	
PP/COC = 75/25; $v_2 = 0.229$									
	$M = 0$			$M = 1$			$M = 1.65$		
4.90	-0.251	0.060	0.9929	-0.263	0.059	0.9935	-0.270	0.058	0.9938
9.80	-0.196	0.059	0.9835	-0.222	0.056	0.9945	-0.236	0.054	0.9950
14.70	-0.138	0.076	0.9850	-0.189	0.067	0.9899	-0.214	0.063	0.9915
19.60	-0.088	0.089	0.9873	-0.168	0.072	0.9938	-0.203	0.067	0.9952
Mean	-0.168	0.071	0.9872	-0.211	0.064	0.9929	-0.231	0.061	0.9939
e.s.d.	0.071	0.014		-0.041	0.007		0.030	0.006	

Table 1. (Continued)

Stress	$\log C^a)$	$n^a)$	$R^2 c)$	$\log C^{*b)}$	$n^{*b)}$	$R^2 c)$	$\log C^{*b)}$	$n^{*b)}$	$R^2 c)$
MPa									
PP/COC = 70/30; $v_2 = 0.276$									
	$M = 0$			$M = 1$			$M = 1.65$		
4.90	-0.316	0.059	0.9920	-0.326	0.058	0.9927	-0.333	0.057	0.9930
9.80	-0.234	0.059	0.9927	-0.257	0.056	0.9940	-0.270	0.054	0.9945
14.70	-0.183	0.065	0.9919	-0.223	0.059	0.9941	-0.244	0.056	0.9949
19.60	-0.136	0.079	0.9886	-0.203	0.067	0.9935	-0.234	0.062	0.9948
Mean	-0.217	0.066	0.9913	-0.252	0.060	0.9936	-0.270	0.057	0.9943
e.s.d.	0.070	0.009		-0.054	0.005		0.045	0.003	
PP/COC = 60/40; $v_2 = 0.372$									
	$M = 0$			$M = 1$			$M = 1.65 (1.98)$		
4.90	-0.300	0.042	0.9924	-0.307	0.042	0.9928	-0.312	0.040	0.9930
9.80	-0.230	0.043	0.9866	-0.248	0.042	0.9894	-0.258	0.040	0.9887
14.70	-0.205	0.048	0.9931	-0.234	0.045	0.9944	-0.249	0.043	0.9949
19.60	-0.165	0.057	0.9889	-0.212	0.051	0.9920	-0.236	0.048	0.9930
Mean	-0.225	0.048	0.9903	-0.250	0.045	0.9922	-0.264	0.043	0.9924
e.s.d.	0.057	0.007		0.041	0.004		0.033	0.004	
PP/COC = 50/50; $v_2 = 0.471$									
	$M = 0$			$M = 1$			$M = 2.02$		
4.90	-0.325	0.034	0.9976	-0.331	0.034	0.9977	-0.336	0.033	0.9978
9.80	-0.270	0.036	0.9930	-0.283	0.039	0.9936	-0.300	0.034	0.9840
14.70	-0.244	0.038	0.9907	-0.265	0.036	0.9918	-0.284	0.035	0.9926
19.60	-0.222	0.044	0.9846	-0.255	0.040	0.9874	-0.281	0.038	0.9891
Mean	-0.265	0.038	0.9915	-0.284	0.037	0.9926	-0.300	0.035	0.9909
e.s.d.	0.044	0.004		0.034	0.003		0.025	0.002	
PP/COC = 25/75; $v_2 = 0.727$									
	$M = 0$			$M = 1$			$M = 2.10$		
4.90	-0.437	0.026	0.9705	-0.440	0.025	0.9710	-0.444	0.025	0.9715
9.80	-0.351	0.020	0.9871	-0.357	0.019	0.9875	-0.363	0.019	0.9879
14.70	-0.336	0.020	0.9907	-0.345	0.020	0.9912	-0.355	0.019	0.9916
19.60	-0.320	0.021	0.9920	-0.333	0.021	0.9926	-0.346	0.020	0.9930
Mean	-0.361	0.022	0.009	-0.369	0.021	0.9856	-0.377	0.021	0.9860
e.s.d.	0.052	0.003		0.049	0.003		0.045	0.003	
COC Topas 8007									
	$M = 0$			$M = 1$					
9.70	-0.418	0.009	0.9646	-0.418	0.009	0.9646			
14.60	-0.393	0.009	0.9603	-0.400	0.009	0.9616			
17.00	-0.411	0.009	0.9339	-0.418	0.009	0.9362			
19.50	-0.374	0.010	0.9734	-0.395	0.010	0.9747			
Mean	-0.399	0.009	0.9581	-0.408	0.009	0.9593			
e.s.d.	0.020	0.001		0.012	0.001				

a)  $C, n$ : parameters of Equation (8) for real time  $t$ .

b)  $C^*, n^*$ : parameters of Equation (9) for "internal" time  $t^*$ .

c)  $R$ : reliability values.

d)  $M$ : strain magnification factor for the amorphous phase of PP from Equation (17) or (18).

e) e.s.d.: estimated standard deviation.

f)  $v_2$ : volume fraction of COC in blends.

limit can be approximately superposed over the whole measured time interval if they are reconstructed for a constant (initial) free volume. The superposed curve generated by using three 100 min tests extends over the interval  $-0.5 < \log t^* [\text{min}] \cong 7$  thus exceeding the experimental time by almost 5 orders of magnitude (the long-term creep

test covers the interval  $-0.5 < \log t^* [\text{min}] \cong 6$ ). As can be seen, a series of short-term creeps can successfully substitute for a long-term measurement.

Creep behaviour of COC is visualised in Figure 4 where three short-term creeps are plotted along with one very long measurement (up to 29 160 min). This behaviour of COC

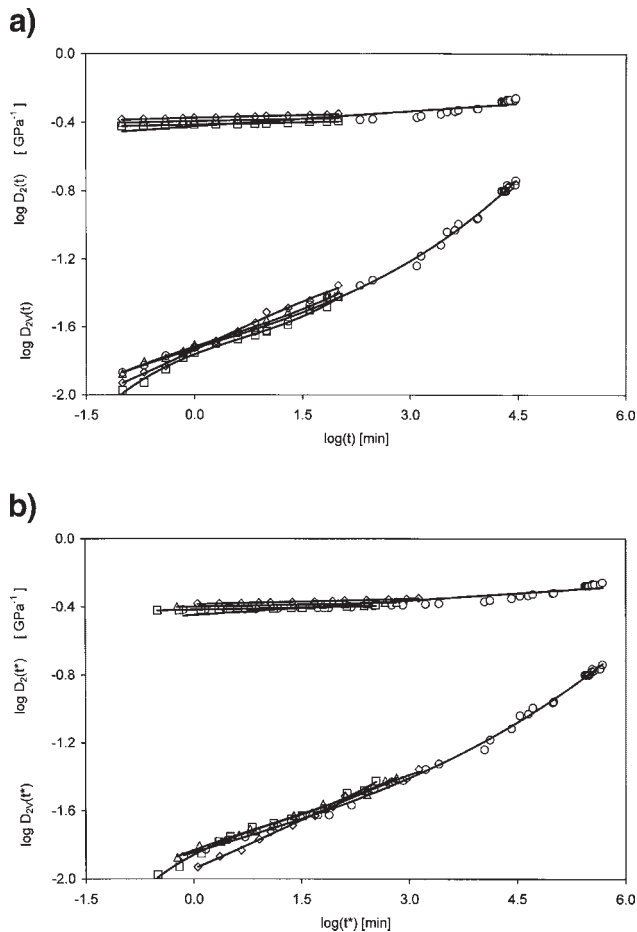


Figure 4. Effect of stress on the compliance  $D(t)$  (upper curves) and viscoelastic component of compliance  $D_v(t)$  (lower curves) of cycloolefin copolymer. Applied tensile stress (MPa): short-term creep: (□) 14.60; (△) 17.00; (◇) 19.50; long-term creep: (○) 17.00. (a)  $M_{1a} = 0$ ; (b)  $M_{1a} = 1$ .

contrasts with that of PP:  $D_2(t)$  is small and practically independent of stress (up to 19.5 MPa) and time; the same holds for  $D_{2v}(t)$ , the level of which is extremely low. If the correction for strain-induced fractional free volume is applied (Figure 4b), the patterns are not markedly affected because the achieved strain and strain-induced free volume are very small. The values  $n$  and  $n^*$  are very low (Table 1) and virtually identical (0.009); also the values  $\log C$  and  $\log C^*$  are close to each other (about  $-0.40$ ) displaying a negligible dependence on applied stress. However, the long-term experiment (Figure 4) indicates some increase in  $n$  or  $n^*$  for long periods of creeping ( $\log t^* > 4$ ).

To reduce the number of figures, analogous experimental results are reported only for the blend PP/COC = 70/30. Figure 5a reveals essential features of the creep behaviour: (i) the blend shows lower compliance than PP because COC fibres form a quasi-continuous phase (in the direction of injection moulding); (ii) the compliances  $D(t)$  and  $D_v(t)$  rise with applied stress, which evidences *non-linear* viscoelastic behaviour in the interval of applied stresses. As soon as

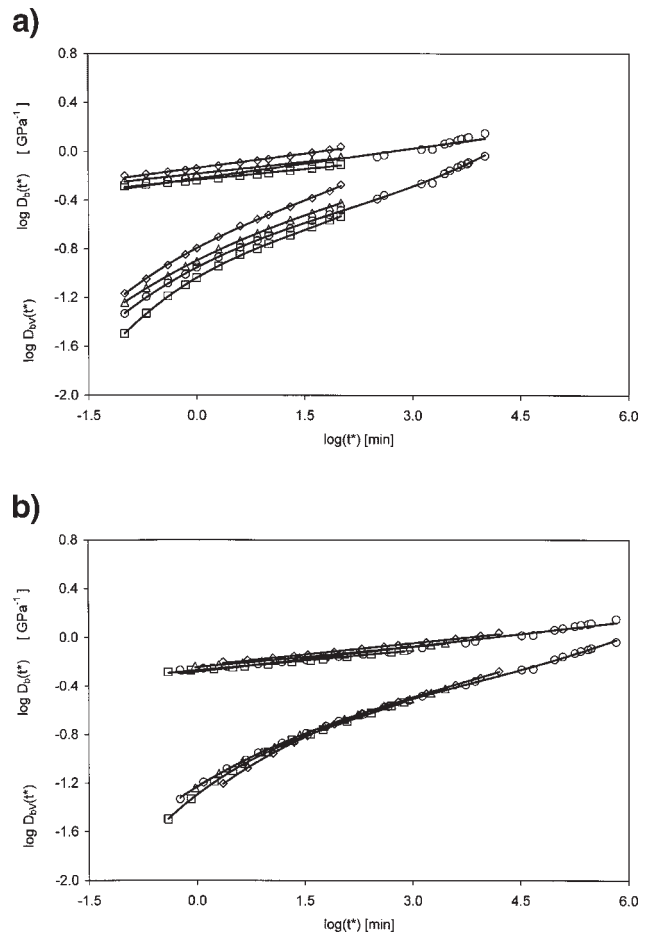


Figure 5. Effect of stress on the compliance  $D_b(t)$  (upper curves) and viscoelastic component of compliance  $D_{bv}(t)$  (lower curves) of PP/COC = 75/25 blend. Applied tensile stress (MPa): short-term creep: (□) 9.80; (△) 14.70; (◇) 19.60; long-term creep: (○) 12.15. (a)  $M_{1a} = 0$ ; (b)  $M_{1a} = 1.65$ .

the strain-induced free volume is taken into account through Equation (10), the dependencies  $\log D_b(t^*)$  vs.  $\log t^*$  or  $\log D_{bv}(t^*)$  vs.  $\log t^*$  found for various stresses superpose (Figure 5b) thus indicating a linear stress-strain relationship in co-ordinates including “internal” time  $t^*$ . As can be seen, superposing dependencies  $\log D(t^*)$  vs.  $\log t^*$  can be fitted by Equation (9).

The effects of four selected stress levels and of parameter  $M_{1a}$  on the extracted parameters  $C$  and  $n$  and on the accuracy of the fitting of experimental data of the time dependencies of  $D(t)$  and  $D_v(t)$  are summarised in Table 1. Replacement of  $M = 0$  by  $M = 1$  brings about a visible decrease in  $C$  and  $n$ . At the same time, the corresponding estimated standard deviation (e.s.d.) is much lower; increased reliability values  $R^2$  confirm that the fitting of experimental data is markedly improved. Introduction of  $M > 1$  calculated from Equation (18) for the amorphous phase of PP leads to further improvement in the fitting procedure manifested by a decrease in e.s.d. and by an increase in  $R^2$ . In parallel, the values of  $\log C^*$  and  $n^*$  display a small reduction. Table 1

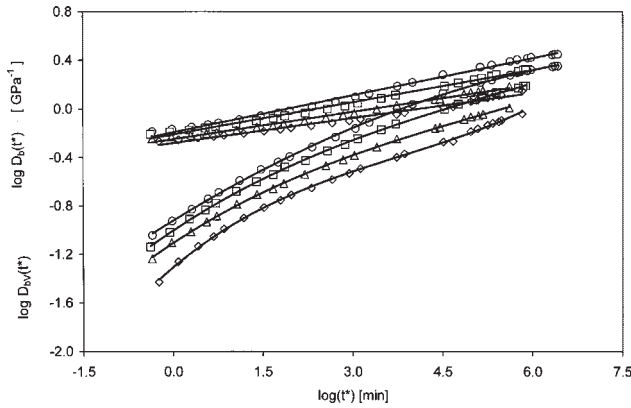


Figure 6. Effect of blend composition on the compliance  $D_b(t)$  (upper curves) and viscoelastic component of compliance  $D_{bv}(t)$  (lower curves):  $M_{1a} = 1.65$ . PP/COC, applied tensile stress (MPa): (O) 100/0, 8.55; (□) 90/10, 8.55; (△) 80/20, 9.76; (◇) 70/30, 12.15.

clearly documents the reinforcing effect of COC in blends manifested as the decrease in their compliance and creep rate.

Long-term creeps of PP, COC and of their blends containing 10–40% of COC are compared in Figure 6 and 7. It is important to note that also the long-term  $\log D(t^*)$  vs.  $\log t^*$  plots can be plausibly approximated by straight lines, while  $\log D_v(t^*)$  with  $\log t^*$  have to be fitted by empirical polynomials of the second order. The figures quantitatively document that the rising fraction of COC in blends accounts for a decrease in (i) compliance  $\log D_b(t^*)$  or  $\log D_{bv}(t^*)$  and (ii) the slope of the  $\log D(t^*)$  vs.  $\log t^*$  plot, i.e. the creep rate.

### Prediction of the Time-Dependent Compliance of Blends in the Non-Linear Stress-Strain Region

On the basis of the acquired knowledge we can predict<sup>[22]</sup> compliance of blends by means of experimental data for

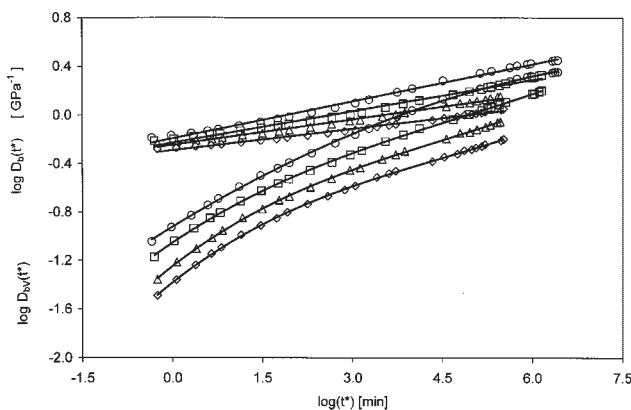


Figure 7. Effect of blend composition on the compliance  $D_b(t)$  (upper curves) and viscoelastic component of compliance  $D_{bv}(t)$  (lower curves):  $M_{1a} = 1.65$ . PP/COC, applied tensile stress (MPa): (O) 100/0, 8.55; (□) 85/15, 9.74; (△) 75/25, 10.98; (◇) 60/40, 12.21.

parent polymers, i.e.,  $\log D_1 = \log C_1^* + n_1^* \log t^*$  and  $\log D_2 = \log C_2^* + n_2^* \log t^*$ . Assuming the validity of  $\log D_b = \log C_b^* + n_b^* \log t^*$  also for blends and introducing these relations into Equation (13), we can obtain the relation between  $C_1^*$ ,  $C_2^*$  and  $C_b^*$  (for  $t = 1$ ):

$$C_b^* = [(v_{1p}/C_1^*) + (v_{2p}/C_2^*) + (v_{1s} + v_{2s})^2 / (v_{1s}C_1^* + v_{2s}C_2^*)]^{-1} \quad (19)$$

The compliance of a blend is then given as

$$\log D_b(t^*) = \log\{[(v_{1p}/C_1^*t^{*y}) + (v_{2p}/C_2^*t^{*z}) + (v_{1s} + v_{2s})^2 / (v_{1s}C_1^*t^{*y} + v_{2s}C_2^*t^{*z})]^{-1}\} = \log C_b^* + n_b^* \log t^* \quad (20)$$

where  $y = n_1^*$  and  $z = n_2^*$ . The relation between  $n_1^*$ ,  $n_2^*$  and  $n_b^*$  assumes the following form:

$$n_b = \{-\log C_b^* - \log[(v_{1p}/C_1^*t^{*y}) + (v_{2p}/C_2^*t^{*z}) + v_s^2 / (v_{1s}C_1^*t^{*y} + v_{2s}C_2^*t^{*z})]\} / \log t^* \quad (21)$$

where  $v_s = v_{1s} + v_{2s}$ . Equation (21) indicates that the parameter  $n_b^*$  predicted by the EBM is a function of the creep time though  $n_1^*$  and  $n_2^*$  are assumed to be time-independent constants; however, the decrease in calculated  $n_b^*$  with the creep time is negligible.<sup>[22]</sup>

Although Table 1 shows that experimentally found values of  $\log C_1^*$ ,  $n_1^*$ ,  $\log C_2^*$  and  $n_2^*$  slightly depend on stress, we will use average values  $\log C_1^* = -0.141 \text{ GPa}^{-1}$ ,  $n_1^* = 0.090$  (for  $M_{1a} = 1.65$ ) and  $\log C_2^* = -0.408 \text{ GPa}^{-1}$ ,  $n_2^* = 0.009$  (for  $M_2 = 1$ ). Table 2 compares experimental data with those calculated by means of the rule of mixtures and the EBM. (Equations corresponding to the rule of mixtures are obtained by introducing  $v_{2s} = 0$  into Equation (19)–(21).) It is evident that the values of  $C_b^*$  and  $n_b^*$  calculated from the rule of mixtures are in a better accord with experimental values (even for  $v_2 > 0.4$ ) than corresponding values from the EBM, which is in conformity with the conclusions of the microscopic analysis.<sup>[45]</sup>

An essential feature of the proposed format is that it makes possible to predict the dependency  $\log D_b(t)$  vs.  $\log t$  for a selected stress (in the interval up to the yield stress) and blend composition. Pre-calculated parameters  $\log C_b^*$  and  $n_b^*$  (Table 2) permit to calculate compliance  $D_b(t^*)$  for a selected “internal” time  $t^*$  given by Equation (10). To obtain a plot of  $\log D_b(t)$  against corresponding “real” time  $t$ , we can modify Equation (7) by introducing  $\varepsilon(t) = \sigma D(t)$ :

$$\log a_\varepsilon = -(B/2.303)[(1 - 2v)M\sigma D(t)/(f_g + \Delta f_{Tc})] / [(1 - 2v)M\sigma D(t) + (f_g + \Delta f_{Tc})] \quad (22)$$

Then, according to Equation (6),

$$\log t = \log t^* + \log a_\varepsilon \quad (23)$$

In this way we can calculate data points of the  $\log D_b(t)$  vs.  $\log t$  curve for a selected tensile stress  $\sigma_b$  employing the

Table 2. Parameters  $C_b^*$  and  $n_b^*$  of Equation (9) extracted from short-term creep experiments or calculated from Equation (19) and (21) for PP/COC blends.

Volume fraction of COC	Experiment		Rule of mixing <sup>a)</sup>		Equivalent box model <sup>b)</sup>	
	$C_b^*$	$n_b^*$	$C_b^*$	$n_b^*$ 100 min	$C_b^*$	$n_b^*$ 100 min
	$\text{GPa}^{-1}$		$\text{GPa}^{-1}$		$\text{GPa}^{-1}$	
0.090	0.681	0.078	0.671	0.075		
0.136	0.625	0.075	0.648	0.069		
0.182	0.614	0.068	0.626	0.063	0.651	0.078
0.229	0.587	0.061	0.605	0.058	0.633	0.075
0.276	0.537	0.057	0.585	0.053	0.616	0.072
0.372	0.544	0.043	0.549	0.044	0.581	0.063
0.471	0.501	0.035	0.516	0.036	0.546	0.054
0.727	0.420	0.021	0.447	0.021	0.464	0.031

<sup>a)</sup> Rule of mixing:  $v_{1s} = v_{2s} = 0$  in Equation (19) and (21).

<sup>b)</sup> EBM:  $v_{1cr} = v_{2cr} = 0.16$ ;  $q = 0$  in Equation (14).

same input parameters  $B$ ,  $M$ ,  $v$ ,  $T_g$ ,  $f_g$ ,  $\Delta f_{Tc}$ ,  $\alpha_{fv}$  previously used in Equation (7), (9) and (10). By using the calculated constants  $C_b^*$  and  $n_b^*$  (Table 2) we can verify the reliability of the prediction of long-term compliance. In Figure 8, compliance of the blend PP/COC = 75/25 predicted for  $\sigma_b = 11$  MPa is compared with the experimental compliance obtained for the same tensile stress. As can be seen, the calculated curve is rather close to a straight line: the anticipated compliance is somewhat higher than experimental data up to  $\log t = 2.5$  while at longer periods the trend is opposite. The reason for the latter difference consists in the fact that experimental dependencies  $\log D = \log C^* + n^* \log t^*$  are not exactly linear and for  $\log t^* > 4$ , the compliance of PP or of blends with  $v < 0.4$  shows a small upswing (cf. Figure 6 and 7). One of possible reasons may consist in the redistribution of the stress acting on the blend fractions (cf. Figure 1) in the course of creep, which accounts for rising

stress acting on the fraction  $v_{2p}$  in Figure 2 (detailed analysis of this phenomenon is given in ref. [22]).

## Conclusions

Additional free volume generated by tensile deformation in thermoplastics with Poisson's ratio smaller than 0.5 accounts for the fact that tensile creep under constant stress and temperature is a non-iso-free volume process. Fractional free volume steadily rising in proportion to the creep strain brings about a continuous shortening of retardation times. The resulting effect can be formally viewed as if the "internal" time  $t^*$  were elapsing "faster" than the real experimental creep time  $t$ . Therefore, the shift factor along the time scale in the time-strain superposition is not constant for a creep curve, but monotonically changes from point to point with the elapsed creep time.

To describe the effects of time and stress on compliance  $D_1(t^*)$  of PP,  $D_2(t^*)$  of COC and  $D_b(t^*)$  of blends, a routinely used empirical equation has been found suitable, which facilitates the manipulation with experimental data. Dependencies  $\log D(t^*)$  vs.  $\log t^*$  or  $\log D_v(t^*)$  vs.  $\log t^*$  obtained for various stresses approximately obey the time-strain superposition thus forming generalised creep curves (over extended time scale) related to a pseudo iso-free volume state. Thus the generalised curve can be constructed by using several short-term creep tests at elevated stresses, which leads to essential saving of experimental time.

Furthermore, the previously proposed predictive format for the time-dependent compliance  $D_b(t^*)$  of polymer blends has been found applicable also to PP/COC blends with fibrous morphology. The  $\log D_b(t^*)$  vs.  $\log t^*$  dependence predicted for a pseudo iso-free-volume state can be transformed into a "real"  $\log D_b(t)$  vs.  $\log t$  curve for a selected stress  $\sigma$  (in the interval up to the yield stress). A comparison of experimental and calculated compliance

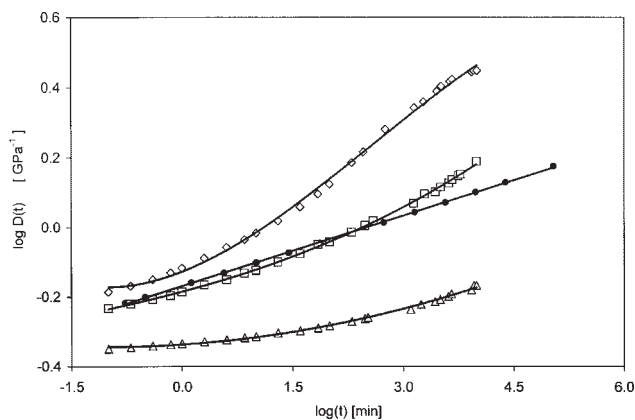


Figure 8. Compliance  $D(t)$  of PP, COC and PP/COC = 75/25 blend as a function of time. Experimental data (composition, stress in MPa): ( $\diamond$ ) PP, 8.55; ( $\triangle$ ) COC, 14.58; ( $\square$ ) 75/25, 11. Data ( $\bullet$ ) calculated from Equation (20) with input parameters  $C_1^* = 0.723 \text{ GPa}^{-1}$ ,  $C_2^* = 0.391 \text{ GPa}^{-1}$ ,  $n_1^* = 0.090$ ,  $n_2^* = 0.009$  (Table 1).

curves for the PP/COC = 75/25 blend shows that the proposed format plausibly predicts the blend creep over the interval 0.1–10 000 min.

**Acknowledgement:** The first author is greatly indebted to the Grant Agency of the Academy of Sciences of the Czech Republic for financial support of this work (Grant No. A4050105). The authors are grateful to Dr. P. Goberti (Basell, Ferrara, Italy) for preparation of blends and test specimens and to Dr. M. Šlouf for taking SEM microphotographs.

- [1] L. E. Nielsen, R. F. Landel, “*Mechanical Properties of Polymers and Composites*”, Marcel Dekker, New York 1994.
- [2] R. J. Crawford, “*Plastics Engineering*”, Butterworth-Heinemann, Oxford 1998.
- [3] F. Bueche, “*Physical Properties of Polymers*”, Interscience, New York 1962.
- [4] N. G. McCrum, B. E. Read, G. Williams, “*Anelastic and Dielectric Effects in Polymeric Solids*”, Wiley, Chichester 1967.
- [5] J. J. Aklonis, W. J. MacKnight, M. Shen, “*Introduction to Polymer Viscoelasticity*”, Interscience, New York 1972.
- [6] I. M. Ward, D. W. Hadley, “*An Introduction to the Mechanical Properties of Solid Polymers*”, Wiley, Chichester 1993.
- [7] F. Rodriguez, “*Principles of Polymer Systems*”, Taylor and Francis, Washington, D.C. 1996.
- [8] J. D. Ferry, “*Viscoelastic Properties of Polymers*”, Wiley, New York 1980.
- [9] E. Riande, R. Diaz-Calleja, M. G. Prolongo, R. M. Masegosa, C. Salom, “*Polymer Viscoelasticity*”, Marcel Dekker, New York 2000.
- [10] C. B. Bucknall, “*Toughened Plastics*”, Applied Science, London 1977.
- [11] L. A. Utracki, “*Polymer Alloys and Blends*”, Hanser Publ., Munich 1990.
- [12] M. J. Folkes, P. S. Hope, “*Polymer Blends and Alloys*”, Chapman and Hall, Cambridge 1993.
- [13] L. H. Sperling, “*Polymeric Multicomponent Materials*”, Wiley, New York 1997.
- [14] L. A. Utracki, “*Commercial Polymer Blends*”, Chapman and Hall, London 1988.
- [15] “*Polymer Blends*”, D. R. Paul, C. B. Bucknall, Eds., Wiley, New York 1999.
- [16] C. B. Bucknall, L. C. Drinkwater, *J. Mater. Sci.* **1973**, *8*, 1800.
- [17] C. B. Bucknall, C. J. Page, *J. Mater. Sci.* **1982**, *17*, 808.
- [18] H. Gramespacher, J. Meissner, *J. Rheol.* **1995**, *39*, 151.
- [19] P. Mariani, R. Frassiné, M. Rink, A. Pavan, *Polym. Eng. Sci.* **1996**, *36*, 2750.
- [20] A. Lee, G. B. McKenna, *J. Polym. Sci., Part B: Polym. Phys.* **1997**, *35*, 1167.
- [21] J. Kolařík, L. Fambri, A. Pegoretti, A. Penati, P. Goberti, *Polym. Eng. Sci.* **2002**, *42*, 161.
- [22] J. Kolařík, A. Pegoretti, L. Fambri, A. Penati, *J. Appl. Polym. Sci.* **2003**, *88*, 641.
- [23] J. Kolařík, *Polym. Eng. Sci.* **1996**, *36*, 2518.
- [24] Z. Horák, J. Kolařík, M. Šípek, V. Hynek, F. Večerka, *J. Appl. Polym. Sci.* **1998**, *69*, 2615.
- [25] J. Kolařík, *Eur. Polym. J.* **1998**, *34*, 585.
- [26] J. Kolařík, A. Pegoretti, L. Fambri, A. Penati, *J. Polym. Res.* **2000**, *7*, 1.
- [27] J. Kolařík, *Polym. Networks Blends* **1995**, *5*, 87.
- [28] J. Kolařík, G. Geuskens, *Polym. Networks Blends* **1997**, *7*, 13.
- [29] J. Kolařík, L. Fambri, A. Pegoretti, A. Penati, *Polym. Eng. Sci.* **2000**, *40*, 127.
- [30] L. A. Utracki, *J. Rheol.* **1991**, *35*, 1615.
- [31] J. Lyngaae-Jorgensen, L. A. Utracki, *Makromol. Chem., Macromol. Symp.* **1991**, *48/49*, 189.
- [32] J. Lyngaae-Jorgensen, A. Kuta, K. Sondergaard, K. V. Poulsen, *Polym. Networks Blends* **1993**, *3*, 1.
- [33] J. Kolařík, *J. Polym. Sci., Part B: Polym. Phys.* **2003**, *41*, 736.
- [34] L. Tritto, L. Boggioni, J. C. Jansen, K. Thorshaug, M. C. Sacchi, D. R. Ferro, *Macromolecules* **2002**, *235*, 616.
- [35] K. Thorshaug, R. Mendichi, L. Boggioni, I. Tritto, S. Trinkle, C. Friedrich, R. Mühlaupt, *Macromolecules* **2002**, *35*, 2903.
- [36] G. Khanarian, *Polym. Eng. Sci.* **2000**, *40*, 2590.
- [37] W. J. Huang, F. C. Chang, P. P. J. Chu, *Polymer* **2000**, *41*, 6095.
- [38] P. P. J. Chu, W. J. Huang, F. C. Chang, *Polymer* **2000**, *42*, 2185.
- [39] T. Scriverani, R. Benavente, E. Perez, J. M. Perena, *Macromol. Chem. Phys.* **2001**, *202*, 2547.
- [40] J. Forsyth, J. M. Perena, R. Benavente, E. Perez, I. Tritto, L. Boggioni, H. H. Brintzinger, *Macromol. Chem. Phys.* **2001**, *202*, 614.
- [41] J. F. Forsyth, T. Scriverani, R. Benavente, C. Marestin, J. M. Perena, *J. Appl. Polym. Sci.* **2001**, *82*, 2159.
- [42] “*Topas (COC)*”, brochure from Ticona, Hoechst, Germany 1995.
- [43] D. Rana, C. H. Lee, K. Cho, B. H. Lee, S. Choe, *J. Appl. Polym. Sci.* **1998**, *69*, 2441.
- [44] J. Luettmmer-Strathmann, J. E. G. Lipson, *Macromolecules* **1999**, *32*, 1093.
- [45] M. Šlouf, J. Kolařík, L. Fambri, *J. Appl. Polym. Sci.*, submitted.
- [46] J. Kolařík, G. L. Agrawal, Z. Kruliš, J. Kovář, *Polym. Compos.* **1986**, *7*, 463.
- [47] T. Matsuoka, S. Yamamoto, *J. Appl. Polym. Sci.* **1998**, *68*, 807.
- [48] R. C. Willemsse, A. P. de Boer, J. van Dam, A. D. Gotsis, *Polymer* **1999**, *39*, 5879.
- [49] R. C. Willemsse, *Polymer* **1999**, *40*, 2175.
- [50] H. Veenstra, J. van Dam, A. P. de Boer, *Polymer* **1999**, *40*, 1190.
- [51] H. Veenstra, P. C. J. Verkooijen, B. B. J. van Lent, J. van Dam, A. P. de Boer, H. J. Nijhof, *Polymer* **2000**, *41*, 1817.
- [52] H. Verhoogt, H. C. Langelaan, J. van Dam, A. P. de Boer, *Polym. Eng. Sci.* **1993**, *33*, 754.
- [53] A. G. C. Machiels, K. F. J. Denys, J. van Dam, A. P. de Boer, *Polym. Eng. Sci.* **1996**, *36*, 2451.
- [54] A. G. C. Machiels, K. F. J. Denys, J. van Dam, A. P. de Boer, *Polym. Eng. Sci.* **1997**, *37*, 59.
- [55] M. F. Boyaud, A. Ait-Kadi, M. Bousmina, A. Michael, P. Cassagnau, *Polymer* **2001**, *42*, 6516.
- [56] M. Evstatiev, J. M. Schultz, S. Fakirov, K. Friedrich, *Polym. Eng. Sci.* **2001**, *41*, 192.
- [57] M. F. Boyaud, P. Cassagnau, A. Michel, *Polym. Eng. Sci.* **2001**, *41*, 684.
- [58] Z. Ling, H. Rui, L. Liangbin, W. Gang, *J. Appl. Polym. Sci.* **2002**, *83*, 1870.
- [59] M. Schlimmer, *Rheol. Acta* **1979**, *18*, 62.
- [60] F. Y. C. Boey, T. H. Lee, K. A. Khor, *Polym. Test.* **1995**, *14*, 425.
- [61] J. X. Li, W. L. Cheung, *J. Appl. Polym. Sci.* **1995**, *56*, 881.

- [62] R. W. Garbella, J. Wachter, J. H. Wendorff, *Prog. Colloid Polym. Sci.* **1985**, 71, 164.
- [63] J. D. Ferry, R. A. Stratton, *Kolloid-Z.* **1960**, 171, 107.
- [64] W. G. Knauss, I. Emri, *Polym. Eng. Sci.* **1987**, 27, 86.
- [65] G. U. Losi, W. G. Knauss, *Polym. Eng. Sci.* **1992**, 32, 542.
- [66] W. G. Knauss, I. J. Emri, *Comput. Struct.* **1981**, 13, 123.
- [67] R. A. Schapery, *Polym. Eng. Sci.* **1969**, 9, 295.
- [68] P. G. de Gennes, *J. Phys., Lett. (Paris)* **1976**, 37, L1.
- [69] W. Y. Hsu, S. Wu, *Polym. Eng. Sci.* **1993**, 33, 293.
- [70] J. Sax, J. M. Ottino, *Polym. Eng. Sci.* **1983**, 23, 165.
- [71] D. W. van Krevelen, “*Properties of Polymers*”, Elsevier, Amsterdam 1997.
- [72] L. Fambri, A. Pegoretti, J. Kolařík, A. Penati, to be published.